J. Biochem. **134**, 843–851 (2003)
DOI: 10.1093/jb/mvg210

Glutamine:phenylpyruvate Aminotransferase from an Extremely Thermophilic Bacterium, *Thermus thermophilus* HB8

Akira Hosono[1], Hiroyuki Mizuguchi[1], Hideyuki Hayashi[1], Masaru Goto[2,3], Ikuko Miyahara[3,4], Ken Hirotsu[3,4] and Hiroyuki Kagamiyama[*,1]

[1]Department of Biochemistry, Osaka Medical College, 2-7 Daigakumachi, Takatsuki 569-8686; [2]Department of Biology, Graduate School of Science, Osaka University, 1-1 Machikaneyama, Toyonaka 560-0043; [3]Department of Chemistry, Graduate School of Science, Osaka City University, 3-3-138 Sugimoto, Sumiyoshi-ku, Osaka 558-8585; and [4]Harima Institute/SPring-8, The Institute of Physical and Chemical Research (RIKEN), 1-1-1 Koto, Mikazuki-cho, Sayo-gun, Hyogo 679-5148

Received August 22, 2003;; accepted September 26, 2003

A subfamily I aminotransferase gene homologue containing an open reading frame encoding 381 amino acid residues (M_r = 42,271) has been identified in the process of the genome project of an extremely thermophilic bacterium, *Thermus thermophilus* HB8. Alignment of the predicted amino acid sequence using FASTA shows that this protein is a member of aminotransferase subfamily Iγ. The protein shows around 40% identity with both *T. thermophilus* aspartate aminotransferase [EC 2.6.1.1] and mammalian glutamine:phenylpyruvate aminotransferase [EC 2.6.1.64]. The recombinant protein expressed in *Escherichia coli* is a homodimer with a subunit molecular weight of 42,000, has one pyridoxal 5′-phosphate per subunit, and is highly active toward glutamine, methionine, aromatic amino acids, and corresponding keto acids, but has no preference for alanine and dicarboxylic amino acids. These substrate specificities are similar to those described for mammalian glutamine: phenylpyruvate aminotransferase. This is the first enzyme reported so far that has the glutamine aminotransferase activity in non-eukaryotic cells. As the presence of aromatic amino acid:2-oxoglutarate aminotransferase [EC 2.6.1.57] has not been reported in *T. thermophilus*, this enzyme is expected to catalyze the last transamination step of phenylalanine and tyrosine biosynthesis. It may also be involved in the methionine regeneration pathway associated with polyamine biosynthesis. The enzyme shows a strikingly high pK_a value (9.3) of the coenzyme Schiff base in comparison with other subfamily I aminotransferases. The origin of this unique pK_a value and the substrate specificity is discussed based on the previous crystallographic data of *T. thermophilus* and *E. coli* aspartate aminotransferases.

Key words: aminotransferase, aromatic-amino-acid, evolution, glutamine, pK_a, pyridoxal, *Thermus*.

Abbreviations: AroAT, aromatic amino acid aminotransferase; AspAT, aspartate aminotransferase; GlnATφ, glutamine:phenylpyruvate aminotransferase; MES, 4-morpholineethanesulfonic acid; PLP, pyridoxal 5′-phosphate; PMP, pyridoxamine 5′-phosphate; TAPS, 3-((tris(hydroxymethyl)methyl)amino)-1-propanesulfonic acid.

Aminotransferases are a group of pyridoxal 5′-phosphate (PLP)–dependent enzymes that catalyze reversible transamination reactions between amino and keto acids by the following ping-pong Bi-Bi mechanism (*1*, *2*), in which the amino group temporarily resides on the cofactor PLP to form pyridoxamine 5′-phosphate (PMP):

$$E_L + \text{amino acid}_1 \leftrightarrow E_M + \text{keto acid}_1 \quad (1)$$

$$E_M + \text{keto acid}_2 \leftrightarrow E_L + \text{amino acid}_2 \quad (2)$$

Here E_L and E_M denote the PLP and PMP forms of the enzyme, respectively.

Aminotransferases are classified into four subfamilies (I–IV) according to their primary structures (*3*). Subfamilies I, II, and IV are distantly related to each other and belong to the same fold type (fold type I; *4*), whereas subfamily III, comprising branched-chain and D-amino acid aminotransferases, has no apparent sequence homology with other subfamilies and belongs to another fold type (fold type IV). Subfamily I aminotransferases have sequence homology with aspartate aminotransferase (AspAT), the most extensively characterized PLP enzyme. Hence subfamily I is often called the "AspAT family." Although AspAT shows high selectivity for dicarboxylic amino and keto acids (aspartate, glutamate, and their corresponding keto acids), the AspAT family comprises aminotransferases that are specific for diverse substrates, such as alanine, aromatic amino acids, histidinol phosphate, *etc*.

In the process of the genome project of an extremely thermophilic bacterium, *Thermus thermophilus* HB8, a gene (C223RA12; open reading frame identification number 1143) homologous to the AspAT family ami-

*To whom correspondences should be addressed. Tel: +81-72-684-7291, Fax: +81-72-684-6516, E-mail: med001@art.osaka-med.ac.jp

notransferases was identified. Based on the sequence homology to alanine aminotransferase, the gene was tentatively named as the "putative alanine aminotransferase gene," but the precise function of the protein remained unclear. To elucidate the function of the protein, we expressed the gene in *Escherichia coli*, purified the product to homogeneity, and physicochemically characterized it. The results showed that the protein is a pyridoxal 5′-phosphate–dependent aminotransferase with a relatively wide range of substrate specificity, and that it resembles the mammalian glutamine: phenylpyruvate aminotransferase (EC 2.6.1.64; glutamine transaminase K, kynurenine aminotransferase I, kynurenine–pyruvate aminotransferase).

EXPERIMENTAL PROCEDURES

Materials—The pET-20b vector was purchased from Novagen (Madison, WI, USA). The *E. coli* BL21-CodonPlus (DE3)-RP competent cells were from Stratagene (La Jolla, CA, USA). Pyridoxamine 5′-phosphate (PMP), 2-aminoadipic acid, 2-oxoadipic acid, L-kynurenine sulfate salt, phenylpyruvic acid, 4-hydroxyphenylpyruvic acid, indolepyruvic acid, and 4-methylthio-2-oxobutyric acid were purchased from Sigma (St. Louis, MO, USA). All other chemicals were of the highest grade commercially available.

Enzyme Assay—The aminotransferase activity was assayed spectrophotometrically as described previously (*5*) with minor modifications. Briefly, enzyme solution was incubated with 10 mM phenylalanine and 5 mM 4-methylthio-2-oxobutyrate in a final volume of 100 μl of 50 mM HEPES–NaOH, 0.1 M KCl, and 0.1 mM EDTA, pH 8.0. After incubation at 25°C for 10 min, 0.9 ml of 3.3 M KOH was added and the absorption at 322 nm was measured (ε = 24,000 $M^{-1}\cdot cm^{-1}$).

Cloning the Gene and Construction of the Expression Vector—Standard cloning techniques were used throughout. The C223RA12 gene was amplified from *T. thermophilus* HB8 genomic DNA using polymerase chain reaction with primers having *Nde*I and *Bgl*II restriction sites. The sequences of the primers were 5′-ATATCATATGCGTCTCCACCCCCGCACCGAGGCGGCCA-3′ (forward primer) with the *Nde*I site (underlined) and 5′-ATATAGATCTTTATTATCCAGATACCGCACCACCTTCGGCT-3′ (reverse primer) with the *Bgl*II site (underlined). The amplified DNA was digested by *Nde*I and *Bgl*II, and the fragment containing the gene was ligated to the *Nde*I and *Bam*HI sites of the pET-20b vector.

Protein Purification—All purification procedures were performed at 4°C. The *E. coli* BL21-CodonPlus (DE3)-RP harboring the pET-20b/C223RA12 gene construct was grown in 10 liters of LB medium containing 50 μg/ml ampicillin and 50 μg/ml chloramphenicol at 37°C with constant shaking at 100 rpm for 24 h. The cells (20 g wet weight) were suspended in 80 ml of buffer A (50 mM potassium phosphate, pH 6.5, 5 mM 2-mercaptoethanol) and disrupted sonically. The cell debris was removed by centrifugation (14,000 ×*g*, 60 min). The supernatant was applied onto a DEAE-Toyopearl 650M column (Tosoh, Tokyo) (2.5 × 20 cm) equilibrated with buffer A. Proteins were eluted with 1 l of a linear gradient of 0–0.3 M NaCl in buffer A. The active fractions were pooled, ammonium sulfate was added to 20% saturation, and the mixture was centrifuged at 14,000 ×*g* for 30 min. The supernatant was applied onto a Phenyl-Toyopearl 650M column (2.5 cm × 20 cm) equilibrated with buffer B (10 mM potassium phosphate, pH 7.0, 5 mM 2-mercaptoethanol) containing 20% ammonium sulfate. Proteins were eluted with 1 l of a linear gradient of 20–0% ammonium sulfate in buffer B. The active fractions were examined by SDS-PAGE. The high purity fractions were pooled, concentrated, sterilized by filtration, and kept at 4°C for short-term storage. The protein was equilibrated with 50 mM HEPES–NaOH buffer (pH 8.0) containing 0.1 M KCl and 0.1 mM EDTA by gel filtration using a PD-10 column (Amersham Biosciences, Uppsala, Sweden) prior to use.

Analytical Methods—The concentration of the pure C223RA12 protein subunit in solution was determined spectrophotometrically using the molar extinction coefficients ε_M = 36,800 M^{-1} cm^{-1} for the PLP-form of the enzyme and ε_M = 35,500 M^{-1} cm^{-1} for the PMP-form of the enzyme at 280 nm. These values were calculated based upon the molar extinction coefficients of tryptophan and tyrosine as described previously (*6*).

Preparation of the PMP-Form of the Enzyme—The PLP form of the holoenzyme was first converted to the apoenzyme. The enzyme was treated with 10 mM L-methionine for 10 min at 25°C in 50 mM HEPES–NaOH, pH 8.0. Solid ammonium sulfate was added to 70% saturation. Then the suspension was adjusted to pH 3.0 with HCl, and stored at 4°C for 12 h. After centrifugation (10,000 ×*g*, 5 min), the precipitate was taken and dissolved in 50 mM HEPES–NaOH, pH 8.0. The enzyme was passed through a PD-10 column equilibrated with 50 mM HEPES–NaOH, pH 8.0, to yield the apoenzyme. PMP was added to the solution to the final concentration of 10 μM. The solution was incubated for 30 min at 25°C, and passed through a PD-10 column equilibrated with 50 mM HEPES–NaOH, pH 8.0, to yield the PMP form of the enzyme.

Stopped-Flow Spectrophotometry—The half-transamination reactions were followed in an Applied Photophysics (Leatherhead, UK) SX.17MV stopped-flow spectrophotometer at 25°C. The dead time was generally 2.3 ms under a pressure of 500 kPa. The buffer solution contained 50 mM HEPES–NaOH, pH 8.0, with 0.1 M KCl and 0.1 mM EDTA. The changes in the absorption spectrum were analyzed similarly as described previously for the reaction of *E. coli* AspAT with substrates (*6*). The apparent rate constant for the exponential change in absorbance was obtained using the program provided with SX.17MV, and kinetic analysis was carried out using nonlinear regression with the software Igor Pro (WaveMetrics, Lake Oswego, OR, USA). The kinetic parameters were determined using the following equation (*6*):

$$k_{app} = \frac{k_{cat}^{half}[S]}{K_m^{half}+[S]} \quad (3)$$

where k_{app} is the apparent rate constant, K_m^{half} and k_{cat}^{half} are the K_m and k_{cat} values, respectively, for the half-transamination reaction, and [S] is the concentration of amino or keto acids.

Spectrophotometric Analysis—Absorption and fluorescence spectra were measured at 25°C using a Hitachi

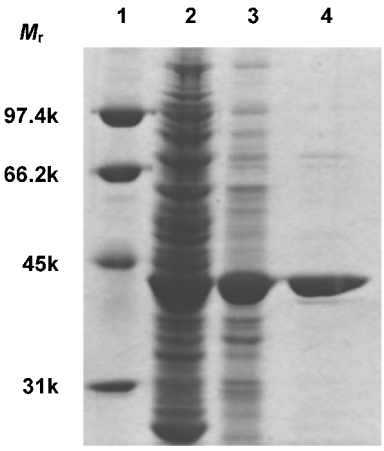

Fig. 1. **Purification of recombinant C223RA12.** 1, marker proteins (the numbers show the molecular weight); 2, crude extract of the transformed *E. coli* cells; 3, after DEAE-Toyopearl 650M; 4, after Phenyl-Toyopearl 650M. The proteins were stained with Coomassie Brilliant Blue R-250.

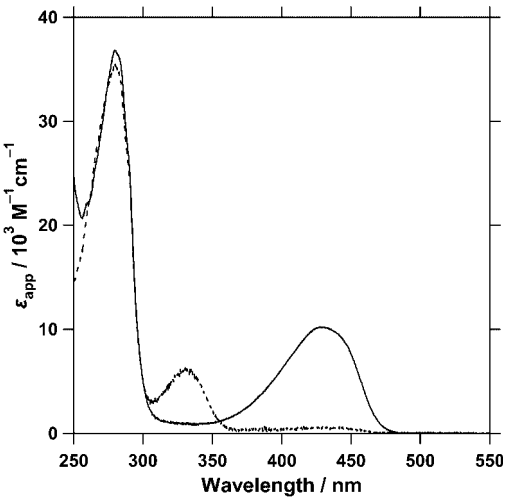

Fig. 2. **Absorption spectra of C223RA12.** Spectra of 10 μM proteins were taken in 50 mM HEPES buffer (pH 8.0) at 25°C. Solid line, PLP form; dashed line, PMP form.

(Tokyo) U-3300 spectrophotometer and 850 fluorescence spectrophotometer, respectively. The buffer solution for absorption measurements contained 50 mM buffer component(s) (MES, HEPES, or TAPS), 0.1 M KCl, and 0.1 mM EDTA. The protein subunit concentration was generally 1–2 × 10^{-5} M.

Phylogenetic Analysis—Amino acid sequences were aligned by using the T-Coffee algorithm (*7*). The phylogenetic tree was constructed using the neighbor-joining method (*8*) with the MEGA2 program (*9*).

Nucleotide Sequence Accession Number—The sequence reported in this paper was submitted to DNA Data Bank of Japan (DDBJ) under accession number AB121092.

RESULTS

Amino Acid Sequence Similarities of the C223RA12 Gene Product—The C223RA12 gene contains an 1,143-base pair open reading frame encoding a protein of 381 amino acids with a predicted molecular weight of 42271. Homology search of the amino acid sequence of the C223RA12 gene product using FASTA (*10*) shows that the protein has high homology with aspartate aminotransferases (AspATs) from *Thermus* [*thermophilus* (41.5% identity; *11*), *aquaticus* (37.1%; *12*)] and other Gram-negative nonproteobacteria, *Deinococcus radiodurans* (33.3%; pir:D75496), *Aquifex aeolicus* (32.6%; sp:AAT_AQUAE), and archea, *Thermoplasma acidophilum* (31.5%; tr:Q9HKR7), *Methanosarcina mazei* (31.2%; tr:Q8Q094), and probable aromatic amino acid aminotransferases (AroATs) from *Pyrococcus horikoshii* (32.4%; *13*), *Methanosarcina acetivorans* (32.2%; tr:Q8TS80), and *Lactococcus plantarum* (30.2%; tr:Q88U47). It shows, however, lower homology with AspAT (*14*) and AroAT (*15*) from *Escherichia coli* (12% and 14%, respectively). Next to AspAT, the protein shows homology with glutamine:phenylpyruvate aminotransferase (EC 2.6.1.64) of eukaryotes including human (36.5%; *16*), and rat (*Rattus norvegicus*) (34.2%; *17*).

Cloning, Overexpression, and Purification—The C223RA12 gene is abundantly expressed in *E. coli* BL21-CodonPlus (DE3)-RP cells, and the C223RA12 protein amounts to about 10% of the total protein in the crude extract of *E. coli*. The recombinant C223RA12 is purified to homogeneity by sequential chromatography on DEAE-Toyopearl and Phenyl-Toyopearl columns, and the purified protein shows a single band with an apparent molecular weight of 42,000 on SDS-PAGE (Fig. 1). The protein also shows a single peak on gel filtration on Sephacryl S-300 (Amersham Biosciences, Uppsala, Sweden), and the molecular weight of the protein is estimated to be 82,000. Therefore, the expressed protein is considered to form a homodimeric structure. The N-terminal amino acid sequence, analyzed by the Hewlett-Packard protein sequencing system G1006A, is Met-Arg-Leu-His-Pro-Arg-Thr-Glu-, which is the same as the deduced N-terminal sequence of the protein.

Spectroscopic Properties—The absorption spectra of the C223RA12 protein purified from *E. coli* are shown in Fig. 2. Beside the absorption maximum at 280 nm, the protein shows a single, large absorption maximum at 430 nm (solid line), indicating the presence of pyridoxal 5′-phosphate (PLP) Schiff base (aldimine). Analysis of the PLP content in the enzyme preparation using the phenylhydrazine method (*18*) shows the presence of 1.05 mol of PLP per mol of subunit. On excitation at 430 nm, the protein shows an intense fluorescence at 500 nm (data not shown), characteristic of the ketoenamine tautomeric form of the protonated PLP aldimine (*19*).

The intensity of 430 nm absorption band decreases, and a new absorption band appears at 352 nm with increasing pH (Fig. 3A). The differential spectrum between the spectra at pH 5.8 and pH 8.7 can be resolved into three lognormal distribution curves (Fig. 3B) (*20*). The major negative band at 434 nm and the minor negative band at 333 nm are assigned to the ketoenamine form and the enolimine form, respectively, of the protonated aldimine (*21*). The positive band at 391 nm is attributed to the unprotonated aldimine (*21*). Therefore, the spectral change is considered to reflect the protonation/deprotonation of the aldimine. The apparent molar

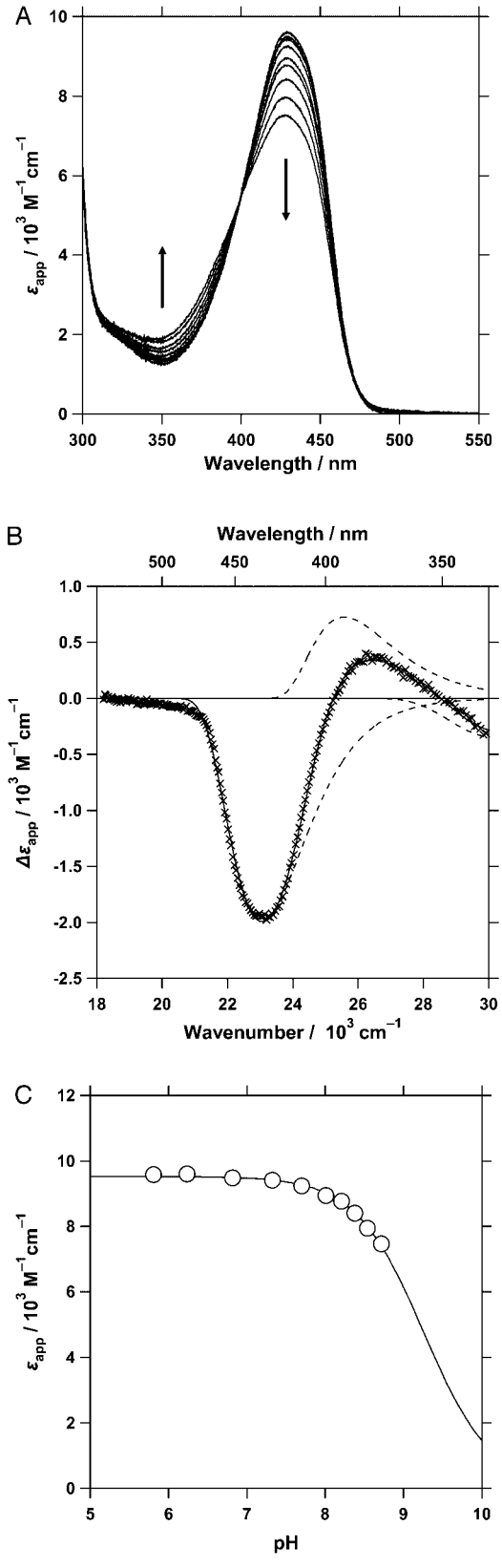

extinction coefficient value of C223RA12 at 430 nm is plotted against pH (shown in Fig. 3C). The apparent pK_a value of the aldimine of C223RA12 is found to be 9.3 by fitting the plots to the following equation:

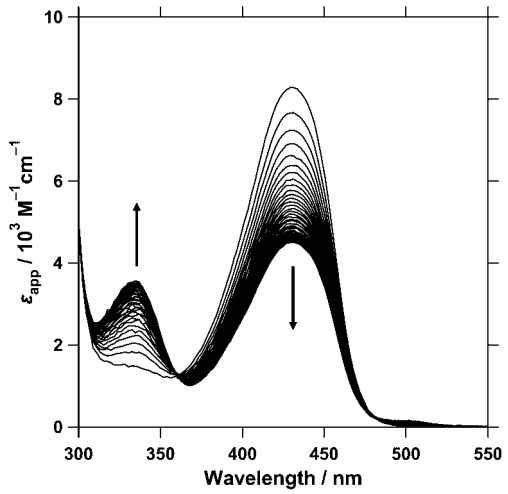

Fig. 4. **Time-dependent spectral change of C223RA12 on reaction with glutamine at pH 8.0, 25 °C.** C223RA12 (50 μM) was reacted with 2 mM glutamine in HEPES buffer (pH 8.0), and the spectral change was monitored using the SX.17MV stopped-flow spectrophotometer equipped with a photodiode array detector at 25°C. Absorption values were collected at 3.84 ms, and every 2.56 ms up to 101.12 ms. The arrows indicate the directions of the spectral changes.

$$\varepsilon_{app} = \varepsilon_E + \frac{\varepsilon_{EH} - \varepsilon_E}{1 + 10^{pH - pK_a}} \quad (4)$$

where ε_E and ε_{EH} denote the molar absorptivity of the unprotonated (E) and protonated (EH) forms of the aldimine, respectively. On calculating the aldimine pK_a, the ε_E value is set to zero, because the unprotonated aldimine has no absorption over 400 nm (*21*). The C223RA12 protein reconstituted with pyridoxamine 5′-phosphate (PMP) shows a peak at 330 nm, which arises from the bound PMP (Fig. 2).

Reaction with Amino Acids—On the addition of glutamine to the PLP form of the C223RA12 protein at pH 8.0, the intensity of the 430 nm absorption band decreases with a concomitant increase in the 330 nm band, indicating the formation of the PMP form of the protein (Fig. 4). Other amino acids show similar spectral changes, although the rate of the change varies with the amino acid. Keto acids react with the PMP form of the C223RA12 protein and show spectral changes in the opposite direction, *i.e.*, increase in the 430 nm band with a concomitant decrease in the 330 nm band (data not

Fig. 3. **A: Absorption spectra of C223RA12 at various pHs.** The arrows indicate the directions of change with increasing pH. pH values are: 5.81, 6.24, 6.82, 7.33, 7.70, 8.01, 8.21, 8.38, 8.54, and 8.72. **B: Deconvolution of differential spectrum between the spectra of C223RA12 at pH 5.8 and pH 8.7.** The differential spectrum, obtained by subtracting the spectrum at pH 5.8 from that at pH 8.7, is shown by ×. The solid line shows the fit of the spectrum to the sum of three lognormal distribution curves, and the component curves are shown as dashed lines. Parameters of the component curves are: $\tilde{\nu}$ = 2.30 × 10^4 cm^{-1}, W = 2.83 × 10^3 cm^{-1}, ρ = 1.49 for the 434 nm band; $\tilde{\nu}$ = 2.56 × 10^4 cm^{-1}, W = 3.05 × 10^3 cm^{-1}, ρ = 1.68 for the 391 nm band; $\tilde{\nu}$ = 3.02 × 10^4 cm^{-1}, W = 3.60 × 10^3 cm^{-1}, ρ = 1.30 for the 333 nm band. The W and ρ values for the 333 nm band are taken from ref. 20 and are fixed. **C: pH dependence of the apparent molar extinction coefficient at 430 nm of C223RA12.** The theoretical line was drawn using Eq. 4.

Table 1. **Kinetic parameters of C223RA12 for the half-transamination reactions with amino and keto acids at pH 8.0 and 25°C and comparison with the overall k_{cat}/K_m values of rat GlnATφ.**

Substrates	C223RA12			Rat GlnATφ[a]
	k_{cat}^{half} (s^{-1})	K_m^{half} (mM)	$k_{cat}^{half}/K_m^{half}$ (s^{-1} M^{-1})	k_{cat}/K_m (s^{-1} M^{-1})
amino acids				
tyrosine	970	0.82	1,200,000	
phenylalanine	590	0.76	780,000	9,900
methionine	1200	3.2	380,000	690
kynurenine	1100	3.2	340,000	
glutamine	830	3.5	240,000	2,500
tryptophan	990	6	170,000	
asparagine	0.13	1	130	
histidine	1.3	18	72	
serine	1.2	37	32	
leucine	1.5	180	8	
alanine	0.18	63	2.9	
glutamate	0.03	21	1.4	
arginine	0.12	130	0.92	
aspartate	0.016	19	0.84	
threonine	0.013	55	0.24	
lysine			N.D.[b]	
glycine			N.D.	
cysteine			N.D.	
isoleucine			N.D.	
valine			N.D.	
proline			N.D.	
2-aminoadipate			N.D.	
keto acids				
4-methylthio-2-oxobutyrate	620	0.14	4,400,000	21,000
4-hydroxyphenylpyruvate	620	0.16	3,900,000	
indolepyruvate	480	0.13	3,700,000	
phenylpyruvate	130	0.06	2,200,000	89,000
pyruvate	15	39	380	
2-oxoglutarate	3.1	25	120	
2-oxoadipate			N.D.	

[a]Parameters for the overall-transamination reactions (*23*). [b]N.D., not detectable.

shown). These observations strongly indicate that the C223RA12 protein functions as an aminotransferase.

Substrate Specificity and Kinetic Analysis—The above spectral changes proceed monoexponentially, and the apparent rate constant (k_{app}) values for the half-transamination reaction are obtained by monitoring the reaction at 430 nm. The kinetic parameters calculated using Eq. 3 are shown in Table 1. C223RA12 is highly specific to glutamine, methionine, and aromatic amino acids including kynurenine. On the other hand, C223RA12 has no preferences for alanine and the dicarboxylic amino acids (aspartate, glutamate, and 2-aminoadipate). The reactivity of keto acids shows a similar tendency to that of the corresponding amino acids (Table 1).

DISCUSSION

Non-Eukaryotic Glutamine: Phenylpyruvate Aminotransferase—The present study demonstrates that the product of the C223RA12 gene of *Thermus thermophilus* HB8 is a homodimeric PLP enzyme that catalyzes transamination between various amino and keto acids. The primary structure shows highest homology with rat mitochondrial glutamine:phenylpyruvate aminotransferase (EC 2.6.1.64; rGlnATφ) as well as *T. thermophilus* HB8 aspartate:2-oxoglutarate aminotransferase (tAspAT), both of which are subfamily Iγ aminotransferases (*22*). The enzyme shows high activity toward glutamine, methionine, aromatic amino acids including kynurenine, and the corresponding keto acids. This substrate specificity is similar to that described for the mitochondrial GlnATφ of rat kidney (Table 1; *23*). Taking these results together, we propose that the product of the gene C223RA12 is GlnATφ. This is the first non-eukaryotic enzyme characterized to date that has the activity of GlnATφ. Hereafter, we call the product of the C223RA12 gene tGlnATφ.

Primary Structure—The amino acid sequence of tGlnATφ is aligned with tAspAT and rGlnATφ in Fig. 5. The residues that have been shown in AspATs from several sources to play important roles in PLP binding, substrate recognition, and catalysis (*3*, *24*) are indicated. Most of these residues are conserved, and some are conservatively replaced in tGlnATφ and rGlnATφ. Accordingly, we can expect the structural and functional roles of some of the residues of tGlnATφ to be as follows (numbers in parenthesis are the corresponding residue numbers of pig cytosolic AspAT (*25*); the numbering is used for eukaryotic and *E. coli* AspATs). Lys222 (258) is the

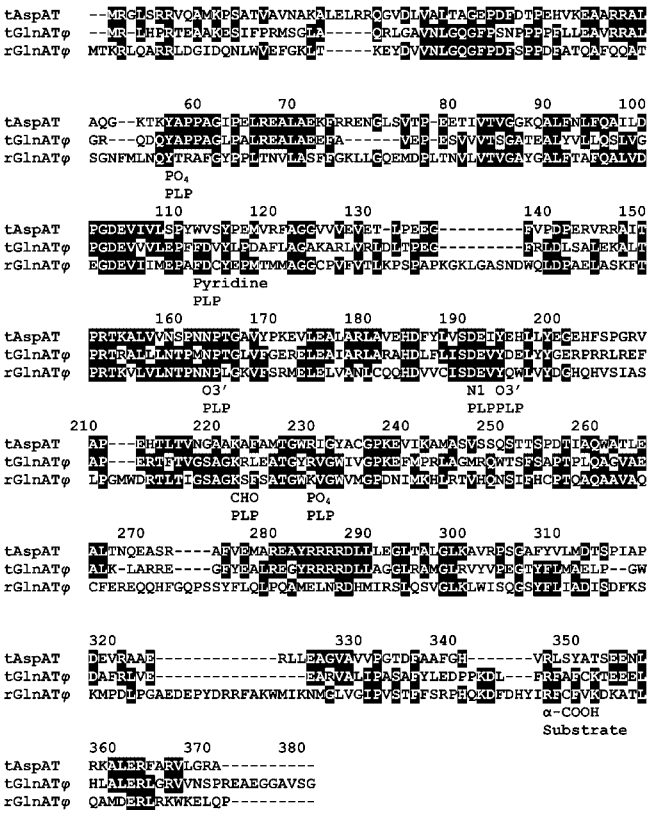

Fig. 5. **Comparison of the amino acid sequences.** Amino acid sequence comparison of *T. thermophilus* glutamine: phenylpyruvate aminotransferase (tGlnATφ) with *T. thermophilus* AspAT [tAspAT, GenBank accession number D38459 (*11*)] and rat mitochondrial GlnATφ [rGlnATφ, GenBank accession number S74029 (*17*)]. The alignment was generated with the T-Coffee algorithm. The black boxes show conserved residues. The numbering of residues corresponds to that of tGlnATφ.

residue whose ε-amino group forms a Schiff base with the aldehyde group of PLP. Asn163 (194) and Tyr194 (225) form hydrogen bonds with O3′ of PLP. Asp191 (222) forms a salt bridge/hydrogen bond with N1 of PLP. Tyr57* (70*) (The asterisk indicates a residue from the other subunit of the homodimer.) forms a hydrogen bond with the phosphate group of PLP. Arg347 (386) is the residue that interacts with the α-carboxylate group of the substrate. Arg230 (266) forms an ion pair with the negatively charged phosphate group of PLP, and contributes to the binding of the coenzyme. This residue, however, is conservatively replaced by Lys in rGlnATφ, showing that the bifurcated hydrogen bonding between the guanidinium and phosphate groups is not a strict requirement for the recognition of the phosphate group.

Conservative replacements of AspAT residues are observed for the residues at 112 (140) and 193 (224) that flank the pyridine ring of PLP. Trp140 and Ala224 of eukaryotic and *E. coli* AspATs are replaced by Trp and Ile in tAspAT, and Phe and Val in tGlnATφ and rGlnATφ, respectively. In *E. coli* AspAT (eAspAT), it has been shown that Phe, but not Gly, can replace Trp140 without affecting k_{cat}, showing that the presence of an aromatic side chain in front of the *re* face of the pyridine ring of PLP is enough for the enzyme to carry out the catalytic process (*26*). However, the Trp140 to Phe replacement significantly increases the K_m values for dicarboxylic substrates without affecting the values for aromatic substrates (*26*). This has been explained as indicating that the hydrogen bonds between the distal carboxylate groups of dicarboxylic substrates with N1 of Trp140 contribute to the binding of dicarboxylic substrates. Crystallographic analysis of the maleate complex of tAspAT shows that this is also the case with tAspAT (*27*). In this regard, it is reasonable to consider that the presence of Trp is not necessary for GlnATφ, which does not recognize dicarboxylic amino or keto acids. The *si* face of the pyridine ring of PLP is occupied by a small methyl group of Ala224 in AspAT (*28* and references therein). This residue is replaced by a bulkier residue Ile in tAspAT (*27*). Figure 6A shows overlaid structures of the active sites of eAspAT and tAspAT. The PLP–Lys258 Schiff base and the surrounding residues are almost superimposed. A significant difference, however, is observed for residue 224. Although tAspAT has a bulky side chain of Ile at this position, Cα of Ile224 is moved in the direction opposite to the coenzyme ring by 0.96 Å as compared to that of Ala224 of eAspAT. Therefore, the pyridine ring of PLP of tAspAT is slightly shifted toward the *si* face. As the result, the PLP–Lys258 Schiff base of tAspAT has a more folded conformation than that of eAspAT. Generally, a folded conformation of the PLP–Lys Schiff base decreases the imine–pyridine torsion angle (C3–C4–C4′–Nζ), and increases the pK_a value of the Schiff base by stabilizing the intramolecular hydrogen bond between O3′ of PLP and Nζ of Lys258 (*29*). However, in tAspAT, the asymmetric side chain of Ile224 causes torsion of the pyridine ring; the ethyl group pushes the C2–C3 part of the pyridine ring (Fig. 6B), and, as the result, the ring is rotated clockwise as viewed from the top in Fig. 6A. This extra torsion is considered to be the cause of the significantly lower pK_a value (6.1) of tAspAT as compared to that of eAspAT (6.8). Interestingly, the residue corresponding to Ile224 of tAspAT is Val in both tGlnATφ and rGlnATφ (Fig. 5). The symmetric side chain of Val will cause the pyridine ring to adopt an orientation similar to that of eAspAT. Furthermore, the reduction in size of the side chain of residue 224 (from Ile to Val) will shift the pyridine ring to the *si* face. The combination of these factors is expected to reduce the imine–pyridine torsion angle of the Schiff base, and may account for the increased pK_a value (9.3) of tGlnATφ.

Insights into the Physiological and Evolutional Aspects—tGlnATφ has high activities toward aromatic amino acids, methionine, and glutamine (Table 1). Considering the substrate specificity of the enzyme and amino acid metabolism in organisms, we can propose the following physiological role of the enzyme. Tyrosine and phenylalanine are synthesized from phenylpyruvate and hydroxyphenylpyruvate, both of which are synthesized in a single step from prephenate, by transamination. The enzyme catalyzing the reaction is aromatic amino acid aminotransferase (EC 2.6.1.57; AroAT) in *E. coli* and other bacteria. However, the presence of AroAT has not been reported in *T. thermophilus*. Therefore, tGlnATφ is considered to catalyze the last step of tyrosine and phenylalanine biosynthesis by using glutamine formed from glutamate and ammonia by glutamine synthetase. Gluta-

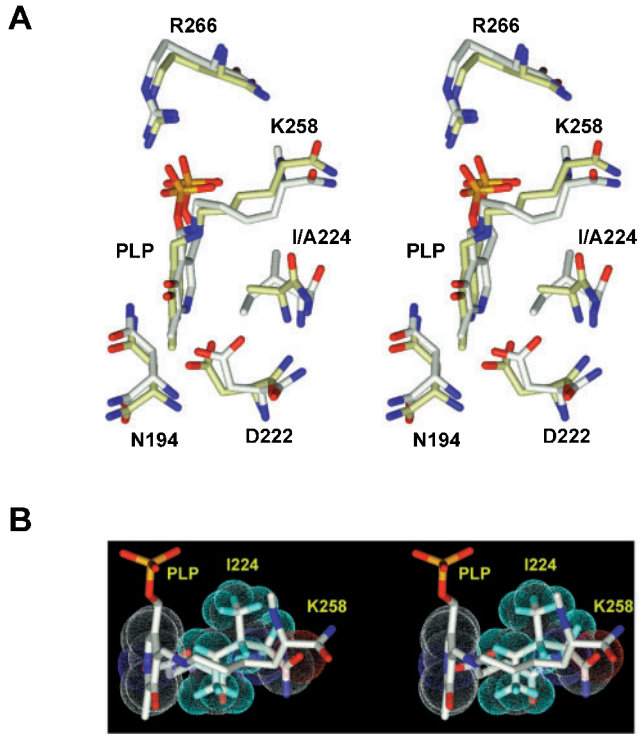

Fig. 6. **A: Superposition of the structures around PLP of tAspAT and eAspAT.** Structures of tAspAT (PDB code: 1BJW; *27*) (carbon atoms in *white*) and eAspAT (PDB code: 1ARS; *28*) (carbon atoms in *khaki*) are aligned at the main chain Cα atoms of the exhibited residues except the residue 222. **B: van der Waals interaction between Ile224 and PLP in tAspAT.** The van der Waals surfaces of Ile224 and the pyridine ring of PLP are displayed with *dots*. The numbering of residues corresponds to that of pig cytosolic AspAT**.** The molecular graphics were drawn using MolMol (*42*).

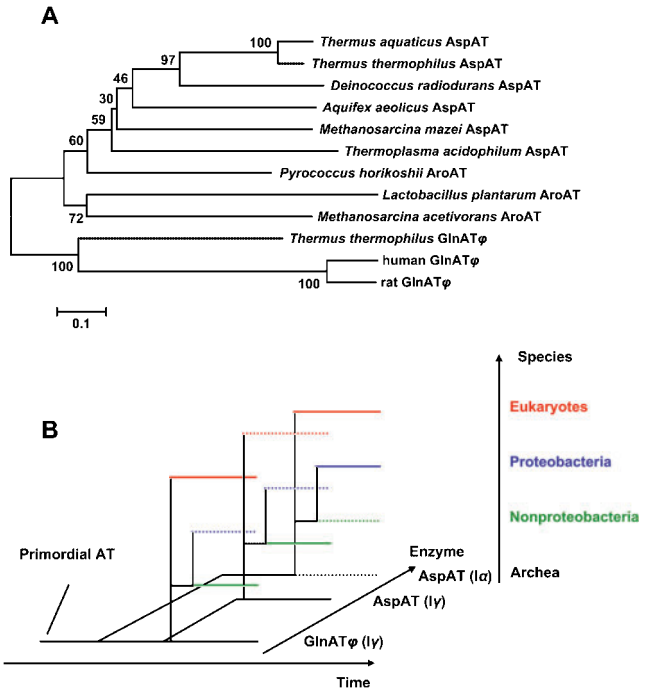

Fig. 7. **A: Phylogenetic tree of the subfamily Iγ aminotransferases.** The selected sequences were aligned with the T-Coffee algorithm and used for the tree construction with the neighbor-joining method. Numbers on selected nodes indicate bootstrap values. **B: Schematic drawing of the divergence of subfamily I aminotransferases.** See text for detail.

mate is synthesized from 2-oxoglutarate and ammonia in general nitrogen-fixation reaction systems. Another interesting point is the activity toward methionine. Methionine is required for a number of important cellular functions, including the initiation of protein synthesis, sulfur metabolism, methyl-transfer reactions, and polyamine synthesis. Large amounts of polyamines are synthesized in rapidly growing cells such as most bacteria, parasites, and tumor cells (*30*, *31*). The production of the polyamines such as spermidine and spermine consumes the decarboxylated *S*-adenosylmethionine as the aminopropyl group donor, yielding 5′-methylthioadenosine as a by-product. In addition to the *de novo* biosynthesis route of methionine from homoserine, there exists a unique pathway that regenerates methionine from 5′-methylthioadenosine, which has been found in organisms ranging from bacteria to mammals (*32*). Transamination to 4-methylthio-2-oxobutyrate is the final step of this pathway. Aminotransferases having activity toward methionine are responsible for this step: AroAT in *Klebsiella pneumoniae* (*32*), branched-chain amino acid aminotransferase [EC 2.6.1.42] in *Bacillus* species (*33*), and AspAT in parasitic protozoa (*34*). In rat liver, where the amount of branched chain amino acid aminotransferase is very low and AspAT has strict substrate specificity toward dicarboxylic amino and keto acids, glutamine or asparagine is the amino donor for this reaction (*35*). Taking into account the abundance (*36*) and the physiological importance (*37*) of polyamines in *T. thermophilus*, it is interesting to consider the possibility that tGlnATφ has a role of catalyzing the final step of the methionine regeneration in this species.

The unexpected finding is that the homologies between tAspAT, tGlnATφ, and rGlnATφ are of the same order (34–42%). This indicates that the divergence of GlnATφ and subfamily Iγ AspAT by gene duplication occurred near the time when bacteria and eukaryotes diverged. To determine which divergence preceded the other, we have drawn a molecular phylogenetic tree of subfamily Iγ aminotransferases that show high homology with tGlnATφ using the neighbor-joining method (Fig. 7A). The tree shows clear separation of the AspAT/AroAT and GlnATφ groups. This indicates that the gene duplication within the Iγ aminotransferases is the earlier event in the evolution.

Combining the above findings with the results of the phylogenetic studies by Jensen and Gu (*22*), we can schematically portray the relationship between the subfamily I aminotransferases as in Fig. 7B. The evolution scenario is as follows. First, there was a primordial aminotransferase that had broad substrate specificity. After gene duplication, subfamily Iα diverged from subfamily Iγ and became specialized to dicarboxylic amino and keto acids (Iα AspAT). Later, gene duplication occurred within subfamily Iγ, and one of the aminotransferases specialized to catalyze the same reaction as the Iα aminotransferases. Thus, there is a convergent evolution of Iα AspAT and Iγ AspAT shown in Fig. 7B. Soon after this gene duplication,

archea, bacteria, and eukaryotes diverged. The first archea may have had the Iα aminotransferase(s), but soon replaced it with a functionally equivalent Iγ AspAT. Bacteria retained the Iα aminotransferase at least until the time when nonproteobacteria and proteobacteria diverged. Nonproteobacteria lost the Iα aminotransferase and came to use Iγ AspAT, in a similar way as archea. Proteobacteria, on the other hand, have preserved the Iα aminotransferase, but lost many of the Iγ aminotransferases. As a Iγ aminotransferase with broad substrate specificity, like GlnATφ, is important for the metabolism of aromatic amino and keto acids, proteobacteria had to develop a Iα substitute for GlnATφ, and this is Iα AroAT. In eukaryotes, the Iα aminotransferases are highly specific to dicarboxylic amino and keto acids. Therefore, aromatic amino and keto acids are metabolized by the Iγ aminotransferases, including tyrosine aminotransferase [EC 2.6.1.5] and GlnATφ. The present study shows the existence of GlnATφ in nonproteobacteria, and reveals the compensatory relationship of the Iα and Iγ aminotransferases among species as shown in Fig. 7B.

In mammals, GlnATφ is identical with kynurenine aminotransferase I (kynurenine: pyruvate aminotransferase; EC 2.6.1.7) (*17*, *38*, *39*), which is known to catalyze transamination of kynurenine to form 4-(2-aminophenyl)-2,4-dioxobutanoate, which then cyclizes to kynurenate. Kynurenate acts as a competitive blocker of the glycine site of the *N*-methyl-D-aspartate receptor and as a non-competitive blocker of the α7 nicotinic acetylcholine receptor (*40*, *41*). In various cerebral diseases such as schizophrenia and Huntington's disease, elevated kynurenate in central nervous system is observed (*40*, *41*). Because of the orthologous homology with mammalian GlnATφ, the structure of tGlnATφ will provide useful information for developing novel therapeutic compounds to control endogenous kynurenate levels. Crystallographic studies on tGlnATφ are now under way in our laboratories.

This work was supported in part by Grants-in-Aid for Scientific Research on Priority Areas (No. 13125101 to H.H. and No. 13125207 to K.H.) from the Ministry of Education, Culture, Sports, Science, and Technology of Japan, and Research Grants (No. 13680697 to H.H. and No. 14580632 to H.M.) from the Japan Society for the Promotion of Science. We thank Drs. Seiki Kuramitsu and Ryoji Masui, Osaka University, for submitting the nucleotide sequence data to DDBJ. C223RA12 is registered as TT0293 in the RIKEN Structural-Biological Whole Cell Project in Japan.

REFERENCES

1. Velick, S.F. and Vavra, J. (1962) A kinetic and equilibrium analysis of glutamic oxaloacetate transaminase mechanism. *J. Biol. Chem.* **237**, 2109–2122
2. Kiick, D.M. and Cook, P.F. (1983) pH studies toward the elucidation of the auxiliary catalyst for pig heart aspartate aminotransferase. *Biochemistry* **22**, 375–382
3. Mehta, P.K. and Christen, P. (2000) The molecular evolution of pyridoxal 5′-phosphate-dependent enzymes. *Adv. Enzymol. Relat. Areas Mol. Biol.* **74**, 129–184
4. Schneider, G., Käck, H., and Lindqvist, Y. (2000) The manifold of vitamin B6 dependent enzymes. *Structure Fold. Des.* **8**, R1–R6
5. Cooper, A.J.L. (1978) Purification of soluble and mitochondrial glutamine transaminase K from rat kidney. *Anal. Biochem.* **89**, 451–460
6. Kuramitsu, S., Hiromi, K., Hayashi, H., Morino, Y., and Kagamiyama, H. (1990) Pre-steady-state kinetics of *Escherichia coli* aspartate aminotransferase catalyzed reactions and thermodynamic aspects of its substrate specificity. *Biochemistry* **29**, 5469–5476
7. Notredame, C., Higgins, D.G., and Heringa, J. (2000) T-Coffee: A novel method for fast and accurate multiple sequence alignment. *J. Mol. Biol.* **302**, 205–217
8. Saitou, N. and Nei, M. (1987) The neighbor-joining method: a new method for reconstructing phylogenetic trees. *Mol. Biol. Evol.* **4**, 406–425
9. Kumar, S., Tamura, K., Jakobsen, I.B., and Nei, M. (2001) MEGA2: molecular evolutionary genetics analysis software. *Bioinformatics* **17**, 1244–1245
10. Pearson, W.R. (2000) Flexible sequence similarity searching with the FASTA3 program package. *Methods Mol. Biol.* **132**, 185–219
11. Okamoto, A., Kato, R., Masui, R., Yamagishi, A., Oshima, T., and Kuramitsu, S. (1996) An aspartate aminotransferase from an extremely thermophilic bacterium, *Thermus thermophilus* HB8. *J. Biochem.* **119**, 135–144
12. O'Farrell, P., Sannia, G., Walker, J.M., and Doonan, S. (1997) Cloning and sequencing of aspartate aminotransferase from *Thermus aquaticus* YT1. *Biochem. Biophys. Res. Commun.* **239**, 810–815
13. Matsui, I., Matsui, E., Sakai, Y., Kikuchi, H., Kawarabayasi, Y., Ura, H., Kawaguchi, S., Kuramitsu, S., and Harata, K. (2000) The molecular structure of hyperthermostable aromatic aminotransferase with novel substrate specificity from *Pyrococcus horikoshii*. *J. Biol. Chem.* **275**, 4871–4879
14. Kuramitsu, S., Okuno, S., Ogawa, T., Ogawa, H., and Kagamiyama, H. (1985) Aspartate aminotransferase of *Escherichia coli*: nucleotide sequence of the *aspC* gene. *J. Biochem.* **97**, 1259–1262
15. Kuramitsu, S., Inoue, K., Ogawa, T., Ogawa, H., and Kagamiyama, H. (1985) Aromatic amino acid aminotransferase of *Escherichia coli*: nucleotide sequence of the *tyrB* gene. *Biochem. Biophys. Res. Commun.* **133**, 134–139
16. Perry, S., Harries, H., Scholfield, C., Lock, E., King, L., Gibson, G., and Goldfarb, P. (1995) Molecular cloning and expression of a cDNA for human kidney cysteine conjugate β-lyase. *FEBS Lett.* **360**, 277–280
17. Mosca, M., Cozzi, L., Breton, J., Speciale, C., Okuno, E., Schwarcz, R., and Benatti, L. (1994) Molecular cloning of rat kynurenine aminotransferase: identity with glutamine transaminase K. *FEBS Lett.* **353**, 21–24
18. Wada, H. and Snell, E.E. (1961) The enzymatic oxidation of pyridoxine and pyridoxamine phosphates. *J. Biol. Chem.* **236**, 2089–2095
19. Zhou, X. and Toney, M.D. (1999) pH studies on the mechanism of the pyridoxal phosphate-dependent dialkylglycine decarboxylase. *Biochemistry* **38**, 311–320
20. Metzler, C.M. and Metzler, D.E. (1987) Quantitative description of absorption spectra of a pyridoxal phosphate-dependent enzyme using lognormal distribution curves. *Anal. Biochem.* **166**, 313–327
21. Kallen, R.G., Korpela, T., Martell, A.E., Matsushima, Y., Metzler, C.M., Metzler, D.E., Morozov, Yu.V., Ralston, I.M., Savin, F.A., Torchinsky, Yu.M., and Ueno, H. (1985) Chemical and spectroscopic properties of pyridoxal and pyridoxamine phosphates in *Transaminases* (Christen, P. and Metzler, D.E., eds.) pp. 37–108, John Wiley & Sons, New York
22. Jensen, R.A. and Gu, W. (1996) Evolutionary recruitment of biochemically specialized subdivisions of Family I within the protein superfamily of aminotransferases. *J. Bacteriol.* **178**, 2161–2171
23. Cooper, A.J.L. and Meister, A. (1981) Comparative studies of glutamine transaminase from rat tissues. *Comp. Biochem. Physiol.* **69B**, 137–145

24. Kirsch, J.F., Eichele, G., Ford, G.C., Vincent, M.G., Jansonius, J.N., Gehring, H., and Christen, P. (1984) Mechanism of action of aspartate aminotransferase proposed on the basis of its spatial structure. *J. Mol. Biol.* **174**, 497–525
25. Ovchinnikov, Y.A., Egorov, C.A., Aldanova, N.A., Feigina, M.Y., Lipkin, V.M., Abdulaev, N.G., Grishin, E.V., Kiselev, A.P., Modyanov, N.N., Braunstein, A.E., Polyanovsky, O.L., and Nosikov, V.V. (1973) The complete amino acid sequence of cytoplasmic aspartate aminotransferase from pig heart. *FEBS Lett.* **29**, 31–34
26. Hayashi, H., Inoue, Y., Kuramitsu, S., Morino, Y., and Kagamiyama, H. (1990) Effects of replacement of tryptophan-140 by phenylalanine or glycine on the function of *Escherichia coli* aspartate aminotransferase. *Biochem. Biophys. Res. Commun.* **167**, 407–412
27. Nakai, T., Okada, K., Akutsu, S., Miyahara, I., Kawaguchi, S., Kato, R., Kuramitsu, S., and Hirotsu, K. (1999) Structure of *Thermus thermophilus* HB8 aspartate aminotransferase and its complex with maleate. *Biochemistry* **38**, 2413–2424
28. Okamoto, A., Higuchi, T., Hirotsu, K., Kuramitsu, S., and Kagamiyama, H. (1994) X-ray crystallographic study of pyridoxal 5′-phosphate-type aspartate aminotransferases from *Escherichia coli* in open and closed form. *J. Biochem.* **116**, 95–107
29. Hayashi, H., Mizuguchi, H., Miyahara, I., Islam, M.M., Ikushiro, H., Nakajima, Y., Hirotsu, K., and Kagamiyama, H. (2003) Strain and catalysis in aspartate aminotransferase. *Biochim. Biophys. Acta* **1647**, 103–109
30. Tabor, C.W. and Tabor, H. (1984) Polyamines. *Annu. Rev. Biochem.* **53**, 749–790
31. Marton, L.J. and Pegg, A.E. (1995) Polyamines as targets for therapeutic intervention. *Annu. Rev. Pharmacol. Toxicol.* **35**, 55–91
32. Heilbronn, J., Wilson, J., and Berger, B.J. (1999) Tyrosine aminotransferase catalyzes the final step of methionine recycling in *Klebsiella pneumoniae*. *J. Bacteriol.* **181**, 1739–1747
33. Berger, B.J., English, S., Chan, G., and Knodel, M.H. (2003) Methionine regeneration and aminotransferases in *Bacillus subtilis*, *Bacillus cereus*, and *Bacillus anthracis*. *J. Bacteriol.* **185**, 2418–2431
34. Berger, L.C., Wilson, J., Wood, P., and Berger, B.J. (2001) Methionine regeneration and aspartate aminotransferase in parasitic protozoa. *J. Bacteriol.* **183**, 4421–4434
35. Backlund, P.S. Jr., Chang, C.P., and Smith, R.A. (1982) Identification of 2-keto-4-methylthiobutyrate as an intermediate compound in methionine synthesis from 5′-methylthioadenosine. *J. Biol. Chem.* **257**, 4196–4202
36. Hamana, K., Niitsu, M., Samejima, K., and Matsuzaki, S. (1991) Polyamine distributions in thermophilic eubacteria belonging to *Thermus* and *Acidothermus*. *J. Biochem.* **109**, 444–449
37. Uzawa, T., Hamasaki, N., and Oshima, T. (1993) Effects of novel polyamines on cell-free polypeptide synthesis catalyzed by *Thermus thermophilus* HB8 extract. *J. Biochem.* **114**, 478–486
38. Malherbe, P., Alberati-Giani, D., Kohler, C., and Cesura, A.M. (1995) Identification of a mitochondrial form of kynurenine aminotransferase/glutamine transaminase K from rat brain. *FEBS Lett.* **367**, 141–144
39. Abraham, D.G. and Cooper, A.J.L. (1996) Cloning and expression of a rat kidney cytosolic glutamine transaminase K that has strong sequence homology to kynurenine pyruvate aminotransferase. *Arch. Biochem. Biophys.* **335**, 311–320
40. Schwarcz, R. and Pellicciari, R. (2002) Manipulation of brain kynurenines: glial targets, neuronal effects, and clinical opportunities. *J. Pharmacol. Exp. Ther.* **303**, 1–10
41. Stone, T.W. and Darlington, L.G. (2002) Endogenous kynurenines as targets for drug discovery and development. *Nat. Rev. Drug Discov.* **1**, 609–620
42. Koradi, R., Billeter, M., and Wüthrich, K. (1996) MOLMOL: a program for display and analysis of macromolecular structures. *J. Mol. Graphics* **14**, 51–55